

## Performance limits of indirectly cryogenically cooled silicon monochromators – experimental results at the APS

Wah-Keat Lee,\* Kamel Fezzaa, Patricia Fernandez, Gordon Tajiri and Dennis Mills

Advanced Photon Source, Argonne National Laboratory, 9700 South Cass Avenue, Argonne, IL 60439, USA.

E-mail: wklee@aps.anl.gov

The results of high-heat-load tests of indirectly cryogenically cooled silicon monochromators are presented. The measurements show that, provided that the total power absorbed by the crystal is less than  $\sim 150$  W, indirect cryogenically cooled silicon monochromators will perform well, with thermal-induced slope errors of less than 2 arcsec. At the Advanced Photon Source, this corresponds to the undulator closed-gap (11 mm) condition at 100 mA with white-beam slit sizes slightly larger than the full width at half-maximum of the radiation central cones. The dependence of the slope errors on the thermomechanical properties of silicon are discussed and clearly demonstrated.

**Keywords:** X-ray optics; high-heat-load optics; cryogenic cooling; silicon monochromators.

### 1. Introduction

Direct cryogenically cooled silicon monochromators are used extensively at the undulator beamlines at the Advanced Photon Source (APS). ‘Direct cooling’ refers to the cases whereby the liquid-nitrogen coolant flows inside the silicon monochromator itself, and is in contrast to ‘indirect cooling’ whereby the liquid nitrogen flows inside a cooling block (*e.g.* a piece of copper) and the silicon monochromator is brought into close thermal contact with the cooling block. The performance limits of direct cryogenically cooled silicon monochromators have been investigated (Lee *et al.*, 2000).

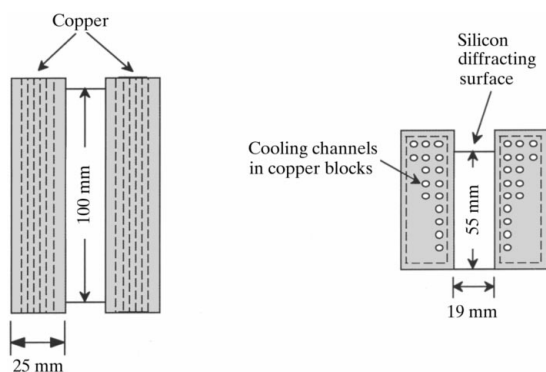


**Figure 1**  
(a) Top and (b) side view of the indirectly cooled crystal, showing the silicon crystal and the cooling blocks.

The results clearly show that direct cryogenically cooled silicon monochromators can successfully handle heat loads that are much higher than those encountered by typical users at current third-generation synchrotron facilities. It is of interest to investigate the possibility of using indirectly cryogenically cooled monochromators because an indirectly cooled system has several advantages. First, the fabrication of directly cooled crystals is much more complicated, time-consuming and costly. Cutting coolant channels into silicon is a relatively slow process. On the other hand, contact-cooled crystals are usually simple rectangular blocks of silicon. Second, directly cooled crystals require a silicon-to-metal-manifold vacuum seal. At the APS, the seals are made with indium foils and metal C-cross-sectional O-rings. Although these seals have been successfully employed, temperature cycling can cause a loss of seal integrity. Furthermore, the process of installing the seal itself is not reliable: it usually takes several attempts before a good vacuum seal is achieved. An indirectly cooled crystal will circumvent the vacuum seal problem because only metal-to-metal seals are required, which are easily accomplished. Indirectly cryogenically cooled monochromators have been tested (Marot *et al.*, 1992) and are being used (Quintana, 2000), but to date no quantitative measurements pertaining to their performance limits have been published.

### 2. Experimental setup

The tests were performed at the SRI-CAT sector 1-ID undulator beamline. The monochromator design is shown in Fig. 1. It is a simple rectangular block of silicon clamped between two cryogenically cooled copper blocks. The copper blocks have 16 3 mm-diameter coolant channels each, as shown in the figure. The estimated clamping pressure on the silicon surfaces was 0.29 MPa. The thermal contact between the silicon and the copper was achieved by using 80% gallium–20% indium eutectic. The silicon contact surfaces were polished (chemical-mechanical slurry), while the copper surfaces were fly-cut but not polished. The copper blocks were nickel-plated to inhibit the indium–gallium from attacking the copper. The crystal was mounted at room temperature before installing into the monochromator tank and cooled. Although the eutectic freezes at cryogenic temperatures, it has the advantage that it wets the silicon and the nickel-plated copper surfaces very well at room temperature. One feature of the design is that the cooling blocks extend above the crystal diffraction surface. This was done as a result of finite-element modelling, which shows that such a design helps dissipate the heat from the crystal surface. The silicon crystal diffracting planes were (111), and the liquid-nitrogen flow rate was  $6.4 \text{ l min}^{-1}$ .

The setup for the experiment is shown in Fig. 2. At the APS, with a standard undulator of period 3.3 cm and length 2.4 m, the full-width-at-half-maximum (FWHM) size of the central cone of the undulator radiation at the monochromator position ( $\sim 28$  m from the source) is  $\sim 1.5$  mm (H)  $\times$  0.5 mm (V). The maximum power density at closed gap (11 mm, undulator deflection parameter  $K = 2.6$ ) at that location is

$\sim 160 \text{ W mm}^{-2}$  at a storage-ring current of 100 mA. The third-order Si(333) reflection at  $\lambda/3$  (I1 ion chamber) was used to measure the amount of thermal-induced slope error on the crystal. In the energy range studied here, the theoretical double-crystal rocking-curve widths of the third-order reflections are less than 1 arcsec; thus, the widths are a good indication of the thermal-induced slope errors. The data will show that the mounting-induced crystal strain is less than 1 arcsec over the beam footprint. The power and power density numbers quoted below and in the figures were calculated from *XOP* (Dejus & del Rio, 1996). Calorimetry was performed to check the accuracy of the calculated numbers; the measured power was  $\sim 10\text{--}20\%$  lower.

### 3. Results and discussion

To investigate the performance limits of the indirectly cryogenically cooled silicon monochromator, the performance of the crystal in the thermal parameter space as defined by the undulator gap, white-beam slit size and angle of the crystal was mapped out. As in a previous publication (Lee *et al.*, 2000), the data will be presented as a plot of the high-order rocking-curve (I1) FWHM width *versus* two thermal variables: the total absorbed power in the crystal and the average (over the beam footprint) absorbed power density in the first 10  $\mu\text{m}$  of silicon. The rationale behind this method of data presentation is discussed below.

Subbotin *et al.* (1988) have shown that for a simple cylindrical model, in which the thermal load,  $Q$  ( $\text{W mm}^{-2}$ ), is absorbed on the surface (normal to the cylindrical axis) and cooled from the opposite surface, the surface slope error,  $\Delta\theta$ , is given by

$$\Delta\theta = F \frac{\alpha}{k}(T) Q, \quad (1)$$

where  $\alpha$  is the thermal expansion coefficient ( $\text{K}^{-1}$ ),  $k$  is the thermal conductivity ( $\text{W cm}^{-1} \text{K}^{-1}$ ) and  $F$  is a positive constant that depends on the exact geometry of the model (*e.g.* dimensions of the cylinder and the thermal footprint). In this model, all the power is assumed to be absorbed on the surface, and  $Q$  is the absorbed power density on the surface. In reality, this assumption is inaccurate, especially at hard X-ray

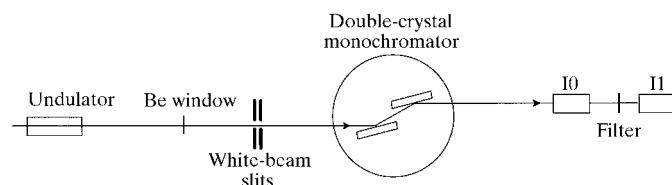


**Figure 2**

Experimental setup. The back ion chamber (I1) is sensitive to the  $\lambda/3$  Si(333) high-order reflection. The distance between the monochromator and the undulator is  $\sim 28$  m, which is typical for APS beamlines.

synchrotrons. At the APS, the critical energy of the beam can be quite high ( $>20$  keV), and a significant amount of power is absorbed deep ( $>2$  mm) in the crystal. To assume that all the power is absorbed on the surface greatly overestimates the thermal distortion. Since extinction lengths in the 8–20 keV range for Si(111) are usually a few micrometres, one possibility is to associate  $Q$  with the average absorbed power density in the first 10  $\mu\text{m}$  (measured along the beam direction) of silicon. (That is,  $Q$  is taken to be the total power absorbed in the first 10  $\mu\text{m}$  of silicon divided by the area of the beam footprint.) Since the absorption lengths here are in the millimeter range, the absorption in the first few tens of micrometres is, to a good approximation, linear. Therefore, there is no need to associate  $Q$  with the average absorbed power density in the exact extinction length of the particular energy, since the value of  $Q$  per unit depth is approximately constant for the first few tens of micrometres. A previous publication (Lee *et al.*, 2000) using this approach has shown that this choice of  $Q$  appears to be reasonable.

Fig. 3 shows a plot of  $\alpha/k$  in the 50–300 K range. In this region,  $\alpha/k$  is well approximated by a polynomial (quadratic or higher). Note that  $\alpha/k$  is negative in the 50–125 K range and positive for  $T > 125$  K. It is reasonable to assume that the average temperature rise in the crystal,  $\Delta T$ , in the vicinity of the thermal load is proportional to the total absorbed power,  $P$ ,

$$\Delta T = bP, \quad T = T_0 + \Delta T, \quad (2)$$

where  $b$  is a positive proportional constant, and  $T_0$  is the initial temperature of the coolant, which in the case of liquid nitrogen is 77 K. Therefore, in this region, assuming that  $\alpha/k$  is approximated by a cubic polynomial,  $\Delta\theta$ , the slope error takes the form

$$\Delta\theta = FQ(c_0 + c_1P + c_2P^2 + c_3P^3), \quad (3)$$

where  $c_0$ ,  $c_1$ ,  $c_2$  and  $c_3$  are constants. Since only the rocking-curve widths are presented, the measurements only reflect the

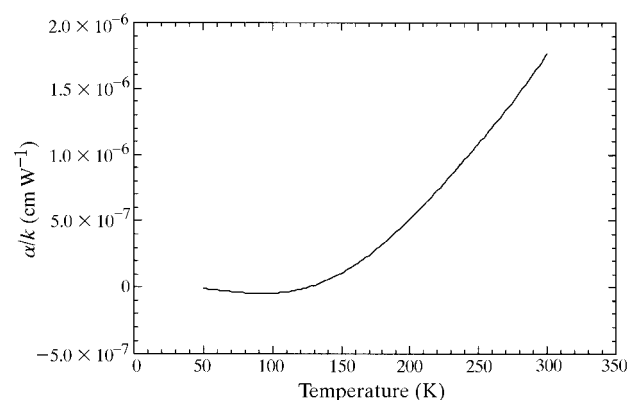


**Figure 3**

Plot of  $\alpha/k$  ( $\text{cm W}^{-1}$ ) for silicon.  $\alpha$  is the thermal expansion coefficient ( $\text{K}^{-1}$ ) and  $k$  is the thermal conductivity ( $\text{W cm}^{-1} \text{K}^{-1}$ ).

absolute values of  $\Delta\theta$ . Thus, equation (3) should be written for current purposes as

$$(\Delta\theta)_{\text{effective}} = FQ|c_0 + c_1P + c_2P^2 + c_3P^3|. \quad (4)$$

Fig. 4 summarizes the performance of the indirectly cryogenically cooled silicon monochromator. As explained above, the FWHM of the Si(333) high-order reflection (I1) is plotted as a function of the total absorbed power and the average absorbed power density in the first 10  $\mu\text{m}$  of silicon. The thin solid line in the plot is a guide to the eye: points to the left and below are places where the FWHM rocking-curve widths are less than or equal to 2 arcsec, while points to the right and above have widths greater than 2 arcsec. The heavy dotted lines are ‘heat-load-tuning curves’, which are the paths within this parameter space that would normally be experienced by an APS user who limits the beam size to the FWHM of the undulator radiation central cone [1.5 mm (H)  $\times$  0.5 mm (V)] and who changes the undulator gaps appropriately such that the first undulator harmonic in the 7–12 keV range and the third undulator harmonic in the 13–20 keV range are used. The results show that the indirectly cryogenically cooled silicon monochromator can be used at APS undulator beam-lines provided that the incoming white-beam size is limited to the FWHM size of the undulator radiation central cone. For ease of comparison and discussion, the data for the directly cryogenically cooled silicon monochromator [using a thick silicon crystal (Lee *et al.*, 2000)] are reproduced in Fig. 5. As expected, the indirectly cooled crystal does not perform as well as the directly cooled crystal.

From equation (4), the lines of constant slope error should thus be hyperbolic-like in shape. This is clearly seen in Fig. 5 in the line separating the I1 FWHM  $\leq$  2 arcsec and the I1 FWHM  $>$  2 arcsec data points. Owing to the added thermal resistance of the indium–gallium interface and the fact that at

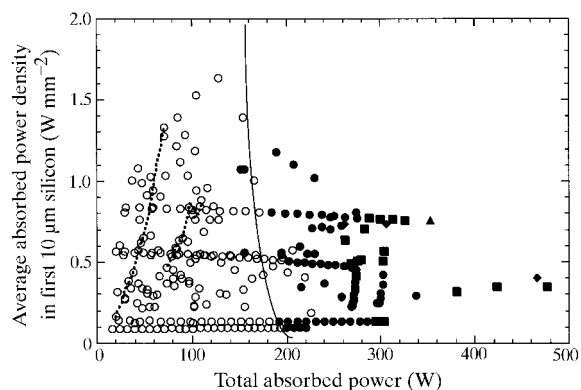


**Figure 4**  
Data for the indirect cryogenically cooled silicon crystal. Open circles denote points with I1 FWHM  $\leq$  2 arcsec, filled circles denote points with 2 arcsec  $<$  I1 FWHM  $\leq$  10 arcsec, filled squares denote points with 10 arcsec  $<$  I1 FWHM  $\leq$  20 arcsec, filled diamonds denote points with 20 arcsec  $<$  I1 FWHM  $\leq$  30 arcsec, and filled triangles denote points with I1 FWHM  $>$  30 arcsec. The heavy dotted line is the ‘heat-load-tuning curve’ (see text) and the thin solid line is a guide to the eye differentiating the ‘good’ and ‘bad’ performance regions.

cryogenic temperatures the conductivity of copper ( $5.6 \text{ W cm}^{-1} \text{ K}^{-1}$ ) is less than that of silicon ( $13.4 \text{ W cm}^{-1} \text{ K}^{-1}$ ), one can expect that, for the same absorbed power, the average temperatures are higher in the indirect cooling case compared with direct cooling. In other words, it should be expected that the proportionality constant,  $b$ , in equation (2), should be larger. The result is that a similar line separating the I1 FWHM  $\leq$  2 arcsec and the I1 FWHM  $>$  2 arcsec data points should move to the left and down in the corresponding plot. In the case of the indirectly cooled crystal, the hyperbolic-like line moves substantially closer to the  $x$ -axis and appears as just a vertical line, as seen in Fig. 4. Thus, the general features of Figs. 4 and 5 can be explained by using this simple thermal model.

Although the simple thermal model is adequate for a qualitative understanding, it is not sufficient for quantitative analysis. Several aspects of the experimental conditions differ significantly from the simple model. First of all, unlike the model, not all the power is absorbed on the surface and a significant amount of power is absorbed millimeters inside the crystal. Second, the geometry of the crystals, both directly and indirectly cooled, are very different from the model. In addition, the data points plotted in Figs. 4 and 5 correspond to many different beam footprints, and thus the factor  $F$  in equation (1) is not a constant for all the data points.

The thermal expansion coefficient of silicon,  $\alpha$ , passes through zero at 125 K. Therefore, the thermal distortions should also show such a minimum at or near 125 K. By keeping the crystal at the same angle, the undulator at the same gap, but changing the size of the horizontal (white-beam) slits, the total power incident (and absorbed) on the crystal can be changed without affecting the peak power density or the spatial-spectral distribution of the beam in the vertical (diffraction) plane. In this way, the average temperature of the crystal can be varied with little or no change to the other parameters. The average absorbed power density in the first

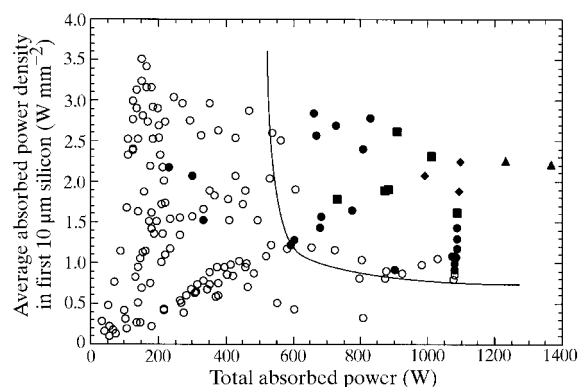


**Figure 5**  
Data for the direct cryogenically cooled thick silicon crystal. Open circles denote points with I1 FWHM  $\leq$  2 arcsec, filled circles denote points with 2 arcsec  $<$  I1 FWHM  $\leq$  10 arcsec, filled squares denote points with 10 arcsec  $<$  I1 FWHM  $\leq$  20 arcsec, filled diamonds denote points with 20 arcsec  $<$  I1 FWHM  $\leq$  30 arcsec, and filled triangles denote points with I1 FWHM  $>$  30 arcsec. The solid line is a guide to the eye differentiating the ‘good’ and ‘bad’ performance regions.

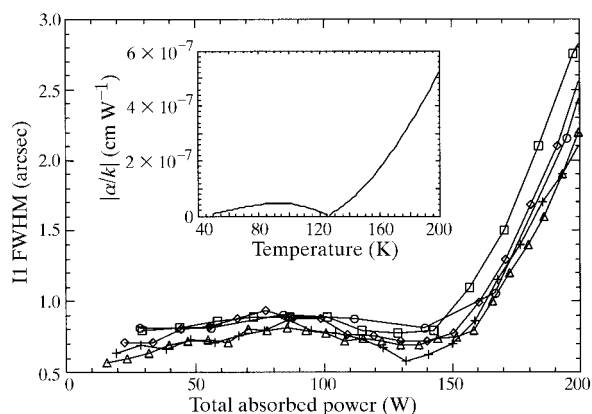


**Figure 6**

Measured high-order rocking-curve widths (I1 FWHM) as a function of total absorbed power. Five sets of data are shown, corresponding to different undulator gaps, crystal angles and filters upstream of the monochromator. Open circles: 11.31 mm gap,  $\theta = 11.4^\circ$ ; open squares: 12.54 mm gap,  $\theta = 9.48^\circ$ ; open diamonds: 12.54 mm gap,  $\theta = 9.48^\circ$ , 1.5 mm carbon filter upstream of the crystal; crosses: 14.68 mm gap,  $\theta = 7.1^\circ$ ; open triangles: 14.68 mm gap,  $\theta = 7.1^\circ$ , 1.5 mm carbon filter upstream of the crystal. The absolute value of  $\alpha/k$  for silicon is shown in the inset.

10  $\mu\text{m}$  of silicon ( $Q$ ) does not change very much when the size of the horizontal slits are changed because of the relatively flat power profile in the horizontal direction. (For the data taken below, the FWHM of the power envelope in the horizontal direction ranged from 8 to 11 mm, while the data were taken with white-beam horizontal slits of 3 mm or less.) Although measuring the actual temperature of the crystal under the beam footprint would be useful, this was not performed due to obvious practical constraints.

Fig. 6 shows the measured high-order rocking-curve widths (I1 FWHM) as a function of total absorbed power. The absolute value of  $\alpha/k$  for silicon is shown in the inset in Fig. 6. Five sets of data are shown, corresponding to different undulator gaps, crystal angles and filters upstream of the

monochromator: (i) 11.31 mm gap,  $\theta = 11.4^\circ$ ; (ii) 12.54 mm gap,  $\theta = 9.48^\circ$ ; (iii) 12.54 mm gap,  $\theta = 9.48^\circ$ , 1.5 mm carbon filter upstream of the crystal; (iv) 14.68 mm gap,  $\theta = 7.1^\circ$ ; (v) 14.68 mm gap,  $\theta = 7.1^\circ$ , 1.5 mm carbon filter upstream of the crystal. The similarity with the inset figure is striking. Note that the minimum (and the small maximum at  $\sim 80$  W) in the rocking-curve measurements all occur at the same total absorbed power under very different thermal load conditions (different beam spectrum and power densities). This reflects the general form of equation (1).

In conclusion, the results show that the indirectly cryogenically cooled silicon monochromator can handle the heat load of the APS undulator A, provided that the white-beam size is limited to the FWHM of the central cone. In particular, the thermal distortions are less than 2 arcsec for total absorbed powers of about 150 W or less. Furthermore, the dependence of the thermal slope errors on the thermo-mechanical figure of merit,  $\alpha/k$ , has been clearly demonstrated.

We would like to acknowledge a fruitful discussion with Andreas Freund and the help of Ali Mashayekhi on the beamline. This work was supported by the US Department of Energy, Basic Energy Sciences, Office of Science, under Contract No. W-31-109-ENG-38.

## References

- Dejus, R. J. & del Rio, M. S. (1996). *Rev. Sci. Instrum.* **67**(9), CD-ROM.
- Lee, W. K., Fernandez, P. & Mills, D. M. (2000). *J. Synchrotron Rad.* **7**, 12–17.
- Marot, G., Rossat, M., Freund, A., Joksche, S., Kawata, H., Zhang, L., Zigler, E., Berman, L., Chapman, D., Hastings, J. B. & Iarocci, M. (1992). *Rev. Sci. Instrum.* **63**(1), 477–480.
- Quintana, J. (2000). Personal communication.
- Subbotin, V. I., Kolesov, V. S., Kuz'Min, Yu. A. & Kharitonov, V. V. (1988). *Sov. Phys. Dokl.* **33**(8), 633–635.